

## Role of the Alkyl–Alkoxide Precursor on the Structure and Catalytic Properties of Hybrid Sol–Gel Catalysts

Alexandra Fidalgo,<sup>†</sup> Rosaria Ciriminna,<sup>‡</sup> Laura M. Ilharco,<sup>\*,†</sup> and Mario Pagliaro<sup>\*,‡</sup>

Centro de Química-Física Molecular, Instituto Superior Técnico, Complexo I, Avenida Rovisco Pais 1, 1049-001 Lisboa, Portugal, and Istituto per lo Studio dei Materiali Nanostrutturati, CNR, via Ugo La Malfa 153, 90146 Palermo, Italy

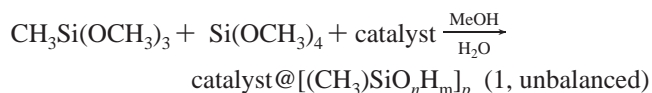
Received September 1, 2005. Revised Manuscript Received October 22, 2005

Detailed diffuse-reflectance infrared Fourier transform structural analysis of a series of organically modified silicates (ORMOSIL)-entrapped catalysts, varying the molar percentage and the alkyl chain length of the organic group, shows that the important factors affording optimal catalytic performance are two: predominance of six-member siloxane rings (above 80% alkylation) and a low hydrophilicity–lipophilicity balance (HLB). These results provide investigators engaged in developing novel catalysts based on the sol–gel route—an advanced chemical technology for synthetic organic/inorganic chemistry—with general guidelines to prepare optimal catalytic materials for a number of relevant applications.

A number of recent studies<sup>1</sup> have proved that catalysts encapsulated in the inner porosity of sol–gel organically modified silicates (ORMOSIL) are much more efficient than other supported catalysts—and even than homogeneous catalysts—in a wide variety of reactions, under largely different conditions. Similarly, ORMOSIL-entrapped enzymes<sup>2</sup> and transition metal complexes<sup>3</sup> are far more efficient (than purely inorganic matrices) at chemical sensing of important analytes.

This superior performance has been correlated with the encapsulation itself (Figure 1) but also with the structure of the sol–gel matrix, namely, the hydrophilicity–lipophilicity balance (HLB) and the textural properties of the materials.<sup>4</sup> The trend was studied and verified, for instance, for reactions catalyzed by transition metal catalysts (TPAP, tetra-*n*-propylammonium perruthenate),<sup>5</sup> organocatalysts (TEMPO,

2,2,6,6-tetramethylpiperidine 1-oxyl radical),<sup>6</sup> and enzyme (lipases)<sup>1b</sup> catalysts entrapped in ORMOSIL prepared by copolymerization of tetramethoxysilane (TMOS) and the modifying co-precursor methyltrimethoxysilane (MTMS):



In all these cases, the resulting sol–gel catalysts are extremely active when compared to catalysis in solution; they show enhanced selectivity and are largely stabilized within the cages of the organosilica gels, allowing separation of the solid catalytic material and efficient recycling.

Moreover, in contrast to zeolites and other crystalline porous solids, such as MCM–silicas that exclude from conversion molecules whose size does not fit that of the pore, those amorphous glassy materials show a distribution of porosity that makes them versatile; i.e., they can be employed in the conversion of structurally different substrates, meeting another key requirement of commercial chemical conversions. It is no surprise that ORMOSIL-entrapped catalysts found immediate application to commercial processes and are now successfully replacing a number of earliest catalytic technologies in the chemical market.<sup>7</sup>

But why are ORMOSIL considerably more active than unmodified silica gels? What are the origins of the performance enhancement, which concerns all the main requirements of a practically useful catalyst (namely, high activity, selectivity, and stability)?

It is the purpose of the present work to understand the role of the modifying alkyl–alkoxide co-precursor in the

\* To whom correspondence should be addressed. E-mail: lilharco@ist.utl.pt (L.M.I.); mario.pagliaro@ismn.cnr.it (M.P.).

<sup>†</sup> Instituto Superior Técnico.

<sup>‡</sup> Istituto per lo Studio dei Materiali Nanostrutturati, CNR.

- (1) A few selected examples. (a) Hydrogenations of emulsified substrates in water: Abu-Reziq, R.; Blum, J.; Avnir, D. *Chem. Eur. J.* **2004**, *10*, 958. (b) Enzymatic esterifications in organic solvent: Reetz, M. T.; Tielmann, P.; Wiesenhofer, W.; Konen, W.; Zonta, A. *Adv. Synth. Catal.* **2003**, *345*, 717. (c) Aerobic oxidations in supercritical carbon dioxide: Campestrini, S.; Carraro, M.; Ciriminna, R.; Pagliaro, M.; Tonellato, U. *Adv. Synth. Catal.* **2004**, *346*, 231. (d) Epoxidations with H<sub>2</sub>O<sub>2</sub>: Campestrini, S.; Donoli, A.; Tonellato, U. *Lett. Org. Chem.* **2004**, *1*, 125. (e) Biocatalytic conversions: Gill, I.; Ballesteros, A. *Trends Biotechnol.* **2000**, *18*, 282. (f) Pandey, P. C.; Upadhyay, S.; Sharma, S. *Electroanal.* **2003**, *15*, 1115. For a recent review on the use of ORMOSIL in catalysis, see: (g) Ciriminna, R.; Pagliaro, M. *Curr. Org. Chem.* **2004**, *8*, 1851. An account on the impressive achievements made possible by the chemistry of doped organo-silica is reported in: (h) Avnir, D.; Klein, L. C.; Levy, D.; Schubert, U.; Wojcik, A. B. *Organo-Silica Sol–Gel Materials*. In *The Chemistry of Organic Silicon Compounds*, Rappoport, Z., Apeloig, Y., Eds.; Wiley: Chichester, U.K., 1998; pp 2317–2362.
- (2) Lee, M.-Y.; Park, C. B.; Dordick, J. S.; Clark, D. S. *Proc. Natl. Acad. Sci. U.S.A.* **2005**, *102*, 983.
- (3) Bukowski, R. M.; Ciriminna, R.; Pagliaro, M.; Bright, F. V. *Anal. Chem.* **2005**, *77*, 2670.
- (4) Ciriminna, R.; Ilharco, L. M.; Fidalgo, A.; Campestrini, S.; Pagliaro, M. *Soft Matter.* **2005**, *1*, 231.
- (5) Ciriminna, R.; Pagliaro, M. *Chem. Eur. J.* **2003**, *9*, 5067.

(6) Ciriminna, R.; Bolm, C.; Fey, T.; Pagliaro, M. *Adv. Synth. Catal.* **2002**, *344*, 159.

(7) Soon commercialized by Fluka after their discovery in 1995, ORMOSIL-entrapped lipases have now reached a second generation of performance; see: Reetz, M. T.; Tielmann, P.; Wiesenhofer, W.; Konen, W.; Zonta, A. *Adv. Synth. Catal.* **2003**, *345*, 717.

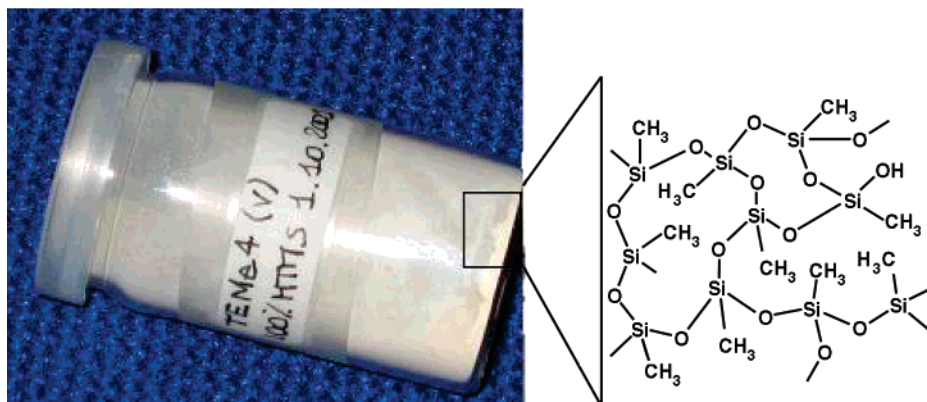


**Figure 1.** Sol-gel ORMOSIL-entrapped TEMPO constitute a new class of highly active heterogeneous catalysts which can be used in a number of selective oxidative conversions.

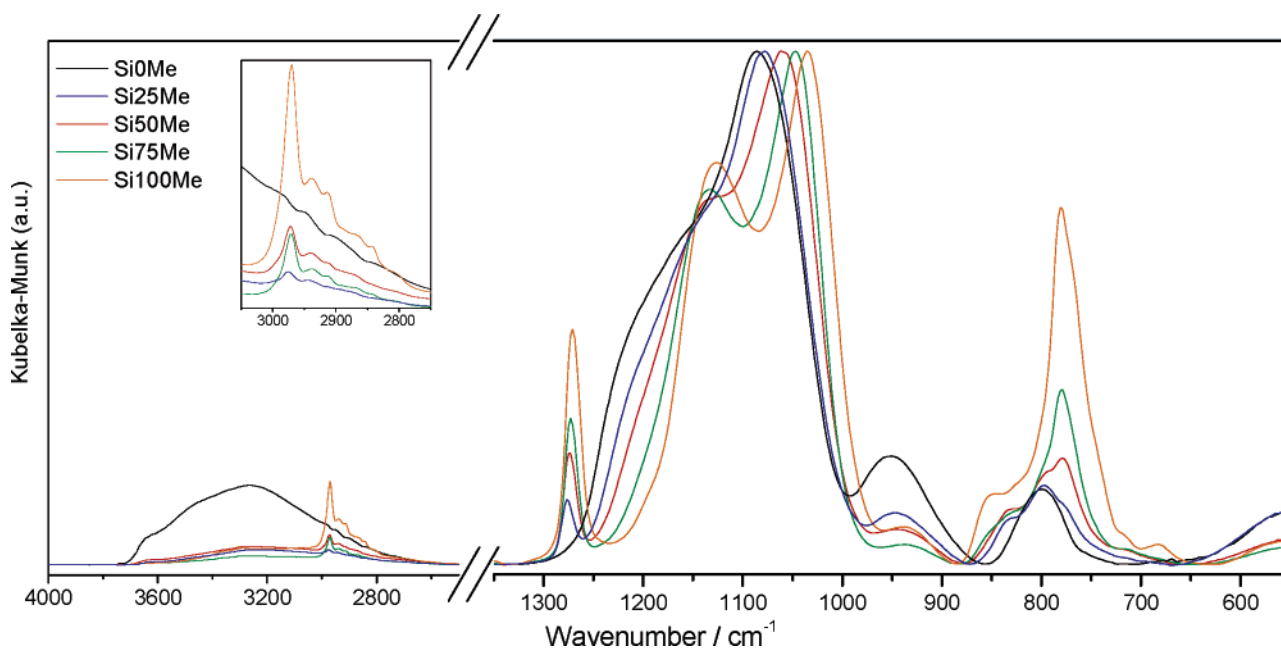


**Figure 2.** DRIFT spectra of silica- and ORMOSIL-entrapped TEMPO on going from 0 (Si0Me) to 100% (Si100Me) methyl-modified xerogels.

structure of the catalyst's hybrid matrix. Two approaches were followed: (i) the effect of the modifier's content was analyzed by varying the molar percentage of MTMS from 0 to 100%; (ii) the effect of the modifier's structure was studied by varying the alkyl chain length from 1 to 3 carbon atoms, for the same composition, namely, using 25% of TMOS (molar) and 75% of methyl-, ethyl-, and propyltrimethoxy-silane (MTMS, ETMS, and PTMS, respectively).

Both approaches aim at correlating the structural modifications induced in the sol-gel matrix with the extraordinary catalytic properties of these materials, taking entrapped TEMPO for oxidation reactions as a model system.

## Results and Discussion

**Influence of the Alkyl-Alkoxide Content.** The DRIFT (diffuse-reflectance infrared Fourier transform) spectra of the sol-gel entrapped TEMPO catalysts prepared with different MTMS contents (from 0 to 100%) are shown in Figure 2. They were normalized to the maximum absorption of the most intense band (centered at  $\sim 1080\text{ cm}^{-1}$  and assigned to the  $\nu_{\text{as}}(\text{Si}-\text{O}-\text{Si})$  mode), to allow comparing the band intensities relative to the silica network. DRIFT spectral

analysis is indeed a powerful tool to investigate the hydrophilicity-lipophilicity balance and the structural properties of sol-gels.<sup>8</sup> The proposed assignments are displayed in Table 1.

The high-wavenumber region of the purely inorganic sample (Si0Me) is very different from the modified ones: the broad band assigned to the  $\nu(\text{O}-\text{H})$  mode, centered at  $\sim 3260\text{ cm}^{-1}$ , is relatively much stronger, evidencing a much higher hydrophilicity of the Si0Me catalyst. In contrast, all the hybrid samples are hydrophobic, as shown by the weak  $\nu(\text{O}-\text{H})$  mode. Since none of the corresponding spectra shows the characteristic deformation mode of molecular water (at  $\sim 1640\text{ cm}^{-1}$ , not shown in Figure 2), the  $\nu(\text{O}-\text{H})$  band is essentially assigned to residual silanol (Si-OH) groups. The small variations in its relative intensity may be related to a slightly different condensation extent for different MTMS contents. For 75%, a *somewhat* less hydrophilic material is obtained.

On the other hand, all the organically modified catalysts are lipophilic, as demonstrated by the presence of  $\nu(\text{C}-\text{H})$

(8) Ilharco, L. M.; Fidalgo, A. *Chem. Eur. J.* **2004**, *10*, 392.

**Table 1.** Assignments of the DRIFT Spectra of the Nonmodified and Modified Sol–Gel Catalysts, with Different MTMS Contents<sup>a</sup>

wavenumber/cm <sup>-1</sup>					
Si0Me	Si25Me	Si50Me	Si75Me	Si100Me	Assignment
3259 <sup>M</sup>	3221 <sup>w</sup>	3228 <sup>w</sup>	3224 <sup>w</sup>	3212 <sup>w</sup>	$\nu(\text{O}-\text{H})$
	2975 <sup>w</sup>	2973 <sup>w</sup>	2972 <sup>w</sup>	2971 <sup>M</sup>	$\nu_{\text{as}}((\text{Si})\text{CH}_3)$
	2941 <sup>vw</sup>	2937 <sup>vw</sup>	2937 <sup>w</sup>	2935 <sup>w</sup>	$\nu_{\text{as}}(\text{O})\text{CH}_3$
			2914 <sup>w</sup>	2911 <sup>vw</sup>	$\nu_{\text{s}}((\text{Si})\text{CH}_3)$
	1277 <sup>w</sup>	1274 <sup>M</sup>	1272 <sup>M</sup>	1270 <sup>S</sup>	$\nu(\text{Si}-\text{C})$
1179 <sup>S</sup>	1155 <sup>S</sup>	1131 <sup>S</sup>	1128 <sup>S</sup>	1123 <sup>S</sup>	$\nu_{\text{as}}(\text{Si}-\text{O}-\text{Si})$
1078 <sup>S</sup>	1069 <sup>S</sup>	1052 <sup>S</sup>	1045 <sup>S</sup>	1034 <sup>S</sup>	$\nu_{\text{as}}\text{Si}-\text{O}-\text{Si}$
945 <sup>M</sup>	943 <sup>w</sup>	939 <sup>w</sup>	943 <sup>w</sup>	938 <sup>w</sup>	$\nu(\text{Si}-\text{O}_d)$
	834 <sup>w</sup>	832 <sup>w</sup>	828 <sup>w</sup>	841 <sup>w</sup>	$\rho(\text{O})\text{CH}_3$
800 <sup>M</sup>	800 <sup>M</sup>	800 <sup>w</sup>			$\nu_{\text{s}}(\text{Si}-\text{O}-\text{Si})$
	774 <sup>M</sup>	777 <sup>M</sup>	778 <sup>M</sup>	775 <sup>S</sup>	$\rho(\text{Si})\text{CH}_3$

<sup>a</sup> S, strong; M, medium; w, weak; vw, very weak; Si–O<sub>d</sub>, dangling oxygen atoms, either as silanol (Si–OH) groups or as broken siloxane bridges (Si–O<sup>-</sup>).

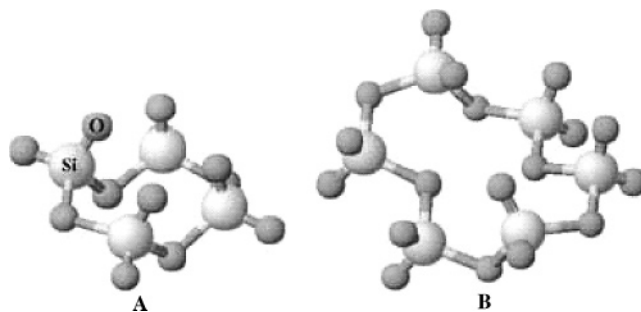
modes in the spectra. The two components of the  $\nu_{\text{as}}(\text{CH}_3)$  band, at  $\sim 2975$  and  $2940\text{ cm}^{-1}$ , were assigned to methyl groups bonded to a silicon and to an oxygen atom, respectively. The relative intensity of the  $\nu_{\text{as}}((\text{Si})\text{CH}_3)$  band clearly increases with the MTMS content, as expected. For samples Si75Me and Si100Me, even the weak  $\nu_{\text{s}}((\text{Si})\text{CH}_3)$  mode becomes visible at 2914 and  $2911\text{ cm}^{-1}$ , respectively, for a sufficiently high amplification of the spectra, as shown in the inset of Figure 2. The weak bands corresponding to the stretching modes of oxygen bonded methyl groups,  $\nu_{\text{as}}(\text{O})\text{CH}_3$ , do not follow the same trend, as an intensity increase with MTMS content is not readily evident from the spectra, which may indicate that the extension of hydrolysis may be affected by the presence of the modifier, but *not* much by its content.

The low-wavenumber region of the spectra ( $500\text{--}1350\text{ cm}^{-1}$ ) contains extremely interesting information on the structural characteristics of the samples, namely, in the  $\nu_{\text{as}}(\text{Si}-\text{O}-\text{Si})$ ,  $\nu(\text{Si}-\text{O}_d)$ , and  $\nu_{\text{s}}(\text{Si}-\text{O}-\text{Si})$  bands, centered at  $\sim 1080$ , 945, and  $800\text{ cm}^{-1}$ , respectively. The band at  $\sim 1270\text{ cm}^{-1}$ , which is absent in the Si0Me spectrum and increases with the MTMS content, was assigned to the  $\nu(\text{Si}-\text{C})$  mode.

The  $\nu_{\text{as}}(\text{Si}-\text{O}-\text{Si})$  band has two observable components, with maxima at  $\sim 1179$  and  $\sim 1078\text{ cm}^{-1}$  (for the pure inorganic sample). As the MTMS content increases, these components shift to lower wavenumbers and their relative intensities change, pointing to major structural differences. Since this band is the silica structural *fingerprint*, a thorough analysis of these modifications involved the band deconvolution into the longitudinal and transverse optical components of the  $\nu_{\text{as}}(\text{Si}-\text{O}-\text{Si})$  mode in the main siloxane ring units (six- and four-member rings), as will be described below.

The  $\nu(\text{Si}-\text{O}_d)$  band, at  $\sim 945\text{ cm}^{-1}$ , which is assigned to the hydrophilic residual silanol groups, confirms the information from the  $\nu(\text{O}-\text{H})$  band: the Si0Me sample contains a much higher proportion of these groups than the hybrid ones, therefore being more hydrophilic. The small differences encountered between the hybrid catalysts were once more attributed to slightly different condensation extents that do not correlate directly with the MTMS content. Again, the 75% modified ORMOSIL is the poorest sample in Si–O<sub>d</sub> groups.

In the  $700\text{--}850\text{ cm}^{-1}$  region of the spectra, the pure inorganic sample contains only one band, at  $800\text{ cm}^{-1}$ ,

**Figure 3.** Schematic diagram of the more common types of primary cyclic arrangements of the structural units, SiO<sub>4</sub>, in xerogels: (A) four-member siloxane ring (SiO<sub>4</sub>) and (B) six-member siloxane ring (SiO<sub>6</sub>).

assigned to the  $\nu_{\text{s}}\text{Si}-\text{O}-\text{Si}$  mode of the silica network. The hybrid catalysts present two additional overlapping bands, at  $\sim 840$  and  $\sim 775\text{ cm}^{-1}$ , that were assigned to the rocking modes of methyl groups ( $\rho(\text{CH}_3)$ ) bonded to an oxygen and to a silicon atom, respectively. The absence of the band at  $840\text{ cm}^{-1}$  in the spectrum of Si0Me reveals that there are *no* unreacted O–CH<sub>3</sub> groups when the precursor is only TMOS; i.e., the hydrolysis reaction is very efficient, a sign of the very high reactivity of this precursor.

When the organic modifier is present, even in a small content, the  $\rho(\text{O})\text{CH}_3$  mode appears in the spectrum, confirming that the hydrolysis extent is affected. The relative intensity of this mode appears to increase slightly with the MTMS content, suggesting a lower reactivity toward hydrolysis of the methoxy groups in MTMS relative to TMOS.<sup>9</sup> On the contrary, the  $\rho((\text{Si})\text{CH}_3)$  band increases noticeably with MTMS content, since the Si–CH<sub>3</sub> groups are not involved in the hydrolysis–condensation reactions.

The band at  $560\text{ cm}^{-1}$ , whose intensity is significant only for the nonmodified and 25% modified samples, and which is assigned to a coupled mode in four-member siloxane rings, (SiO)<sub>4</sub>,<sup>10</sup> provides a qualitative indication that the proportion of these units is relevant in those samples. These siloxane rings, as well as the other common type of rings, (SiO)<sub>6</sub>, are schematized in Figure 3.

For a detailed structural analysis, the ( $\nu_{\text{as}}(\text{Si}-\text{O}-\text{Si}) + \nu(\text{Si}-\text{O}_d)$ ) and the ( $\nu_{\text{s}}(\text{Si}-\text{O}-\text{Si}) + \rho(\text{CH}_3)$ ) spectral regions ( $850\text{--}1300$  and  $700\text{--}850\text{ cm}^{-1}$ , respectively) were independently deconvoluted in Gaussian and Lorentzian components, using a nonlinear least-squares fitting method.<sup>8</sup> The deconvolution profiles for samples Si0Me, Si50Me, and Si100Me are shown in Figure 4.

The peak positions and the integrated areas of the various components are summarized in Table 2 for all the samples. Some relevant ratios between fitted areas are presented in the last rows.

The  $\nu_{\text{as}}(\text{Si}-\text{O}-\text{Si}) + \nu(\text{Si}-\text{O}_d)$  region systematically contains four contributions to the  $\nu_{\text{as}}(\text{Si}-\text{O}-\text{Si})$  band (the longitudinal and transverse optical components of the six- and four-member siloxane rings, LO<sub>6</sub>, LO<sub>4</sub>, TO<sub>6</sub>, and TO<sub>4</sub>), and two components in the  $\nu(\text{Si}-\text{O}_d)$  band (the stretching of the Si–O bond, both in Si–OH and in Si–O<sup>-</sup> groups).

(9) Confirming a well-known feature of organosilanes hydrolytic polymerization. See also: Hüsing, N.; Schubert, U. *Angew. Chem., Int. Ed.* **1998**, *37*, 22.

(10) Hayakawa, S.; Hench, L. J. *Non-Cryst. Solids* **2000**, *262*, 264.

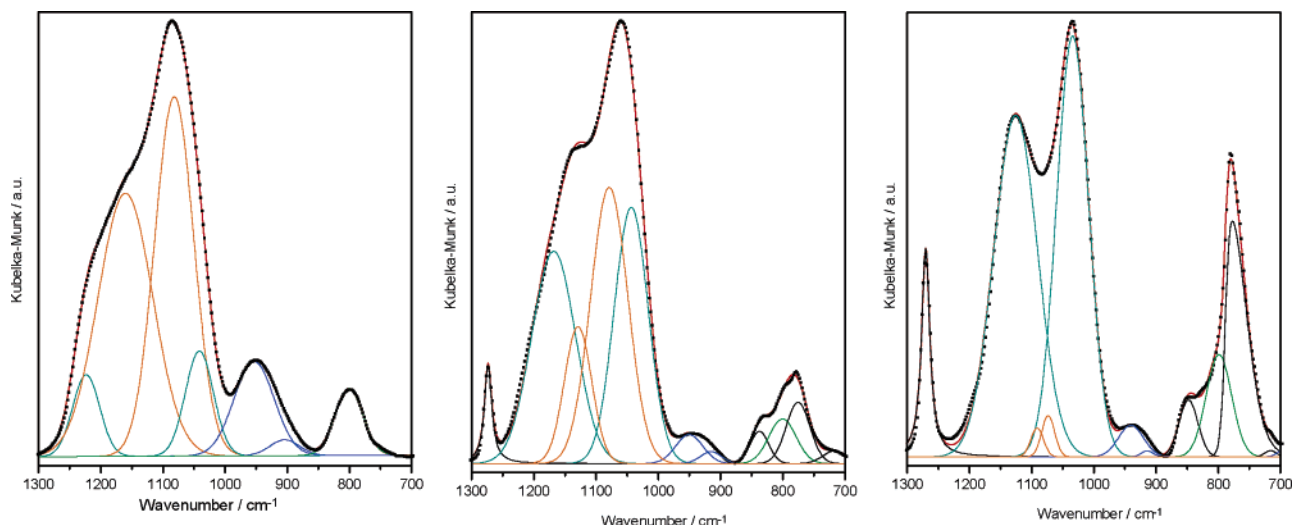


**Figure 4.** Deconvolution of the 850–1300 and 700–850  $\text{cm}^{-1}$  spectral regions for silica- and ORMOSIL-entrapped TEMPO xerogels: Si0Me, Si50Me, and Si100Me.

**Table 2.** Deconvolution of the 850–1300 and 700–850  $\text{cm}^{-1}$  Spectral Regions of the DRIFT Spectra: Position ( $\text{cm}^{-1}$ ) and Integrated Areas (A) of the Components

	Si0Me	Si25Me	Si50Me	Si75Me	Si100Me
850–1300 $\text{cm}^{-1}$					
$\nu(\text{Si}-\text{C})$		1276	1273	1272	1270
A		2.6	5.0	6.5	12.0
$\text{LO}_6$	1223	1214	1168	1138	1126
A	10.2	10.1	42.3	63.6	69.2
$\text{LO}_4$	1160	1149	1129	1102	1091
A	66.6	60.8	17.0	7.0	1.7
$\text{TO}_4$	1082	1077	1079	1070	1074
A	64.7	57.1	46.7	14.3	2.5
$\text{TO}_6$	1041	1040	1044	1041	1034
A	13.6	18.8	39.6	47.8	62.5
$\nu(\text{Si}-\text{OH})$	953	950	951	949	941
A	17.5	6.5	3.6	2.2	3.7
$\nu(\text{Si}-\text{O}^-)$	904	910	916	915	914
A	2.1	1.0	1.1	0.4	0.3
700–850 $\text{cm}^{-1}$					
$\rho((\text{O})\text{CH}_3)$		837	838	841	848
A		1.7	2.7	2.9	5.0
$\nu_s(\text{Si}-\text{O}-\text{Si})$	801	798	801	801	799
A	8.6	7.6	5.5	5.2	12.0
$\rho((\text{Si})\text{CH}_3)$		765	776	776	777
A		0.8	6.6	10.8	47.3
$\%(\text{SiO})_6$	15.3	19.7	56.2	84.0	96.9
$\%\text{Si}-\text{O}_d$	12.6	5.1	3.2	2.0	2.9
$\%(\text{O})\text{CH}_3$		1.1	1.9	2.2	3.7
$\%(\text{Si})\text{CH}_3$		0.5	4.6	8.1	17.4
HLB		3.2	0.5	0.2	0.1

The percentage of six-member rings ( $\%(\text{SiO})_6$ ), first row, last section of Table 2, was estimated as the following ratio of fitted areas:

$$\%(\text{SiO})_6 = 100 \times [A(\text{LO}_6) + A(\text{TO}_6)] / [A(\text{LO}_6) + A(\text{TO}_6) + A(\text{LO}_4) + A(\text{TO}_4)] \quad (2)$$

In the absence of MTMS, the silica structure is dominated by four-member rings (the percentage of six-member units in Si0Me is only  $\sim 15\%$ ), but a spectacular increase in the fraction of six-member rings to 20, 56, 84, and 97% is observed as the MTMS content increases to 25, 50, 75, and 100%. The structure obtained when the precursor is only MTMS is almost entirely formed by the larger, less tensioned, six-member rings, more able to accommodate the unreactive

methyl groups. Interestingly, this correlates with the enhancement in the relative degree of crystallinity (and thus long-range order) that is normally observed in ORMOSIL upon increasing the degree of alkylation of the ceramic matrix.<sup>11</sup>

Another important observation from Figure 4 and Table 2 concerns the positions of the optical components of the  $\nu_{\text{as}}(\text{Si}-\text{O}-\text{Si})$  band: while the LO components are sensitive to the modification ( $\text{LO}_6$  shifts from 1223 to 1126  $\text{cm}^{-1}$  and  $\text{LO}_4$  from 1160 to 1091  $\text{cm}^{-1}$  as the MTMS content increases from 0 to 100%), the TO components show a negligible perturbation. As a consequence, the LO/TO splitting decreases significantly ( $\text{LO}_6/\text{TO}_6$  from 182 to 92  $\text{cm}^{-1}$  and  $\text{LO}_4/\text{TO}_4$  from 78 to 17  $\text{cm}^{-1}$ ). This may be due to the increasing presence of organic groups in the silica network, which are responsible for decreasing the long-range Coulomb interactions that originate the LO/TO splitting.

A possible quantification of the hydrophilicity of the catalyst may be given by the contribution of dangling oxygen atoms relative to the silica structure ( $\%\text{Si}-\text{O}_d$ ). These values, located in the second row in the last section of Table 2, were obtained as

$$\%\text{Si}-\text{O}_d = 100 \times [A(\text{Si}-\text{O}^-) + A(\text{Si}-\text{OH})] / [A(\text{LO}_6) + A(\text{TO}_6) + A(\text{LO}_4) + A(\text{TO}_4)] \quad (3)$$

The relative area of the  $\nu(\text{Si}-\text{O}_d)$  band varies abruptly from  $\sim 13$  to  $\sim 5\%$  when MTMS content is changed from 0 to 25%, but it is not much affected from that content on. Within this slight variation, a minimum may be observed for 75% MTMS. Obviously, the hydrophobicity increases significantly for the organically modified silica gels, and, although it is not very sensitive to the modifier content, it reaches a maximum for 75% MTMS.

On the other hand, a catalytically optimal 75% alkylation degree is required in both ORMOSIL-mediated esterifications<sup>1b</sup> and aerobic oxidations<sup>5</sup> in liquid phase. This experimental outcome indicates that hydrophobicity—that promotes the diffusion of the hydrophobic alcohol and aldehyde molecules

within the porous network—is not the unique factor affecting the reactivity of ORMOSIL-entrapped catalysts; nor is such enhancement due to significant differences in cross-linking between ORMOSIL and unmodified silica xerogels since these differences are small.<sup>12</sup>

The deconvolution of the 700–850 cm<sup>-1</sup> region allows inferring on the main origin of the lipophilic methyl groups in each hybrid catalyst. The contributions from (O)CH<sub>3</sub> and (Si)CH<sub>3</sub> groups, taking the silica network as reference, were estimated by the following ratios:

$$\%(\text{O})\text{CH}_3 = 100 \times [A((\text{O})\text{CH}_3)]/[A(\text{LO}_6) + A(\text{TO}_6) + A(\text{LO}_4) + A(\text{TO}_4)] \quad (4)$$

$$\%(\text{Si})\text{CH}_3 = 100 \times [A((\text{Si})\text{CH}_3)]/[A(\text{LO}_6) + A(\text{TO}_6) + A(\text{LO}_4) + A(\text{TO}_4)] \quad (5)$$

The relative contribution from the  $\rho((\text{O})\text{CH}_3)$  component, at  $\sim 840$  cm<sup>-1</sup>, varies from 1 to 4%, while that of  $\rho((\text{Si})\text{CH}_3)$ , at  $\sim 770$  cm<sup>-1</sup>, varies from 0.5 to  $\sim 17\%$  with increasing MTMS content (third and fourth rows in last section of Table 2). These values substantiate the evolution suggested by observation of the methyl stretching region of the spectra. The hydrolysis extent of the –OCH<sub>3</sub> groups depends on the MTMS content, and therefore on whether they belong to TMOS or MTMS, but the lipophilicity of the modified catalysts is essentially due to the stable, unreactive Si–CH<sub>3</sub> groups.

The DRIFT spectral analysis allows concluding that the presence of the co-precursor MTMS affects the structure and the HLB of the sol–gel catalysts. In the last row of Table 2, a rough estimate of the HLB trend was obtained by the ratio

$$\text{HLB} \approx [A(\text{Si}-\text{O}^-) + A(\text{Si}-\text{OH})]/[A((\text{O})\text{CH}_3) + A((\text{Si})\text{CH}_3)] \quad (6)$$

Although a modification with 25% of MTMS imparts a significant decrease in the catalyst's hydrophilicity without major structural changes, an increase in the MTMS content does *not* affect appreciably the catalyst hydrophilicity, but is responsible for a gradual lipophilicity increase, and therefore for a decrease in the HLB, and for striking structural changes in the silica network.

These findings provide a long awaited solution to the “alkyl effect”<sup>12</sup> for which 800-to-1000% activity enhancements are commonly observed for catalytic species sol–gel entrapped in highly alkylated ORMOSIL matrices, explaining also why, counter to intuition, the gels with the highest diffusional limitations imposed by the narrow pore network still possess the highest reactivity.

As mentioned above, the silica structure made of larger, less tensioned six-member rings is more able to accommodate the unreactive methyl groups; moreover, the alkyl organic groups concentrate at the cage surface,<sup>13</sup> largely diminishing the number of silanols at the surface and, as a consequence, decreasing the intracage hydrogen bonds, which limit the

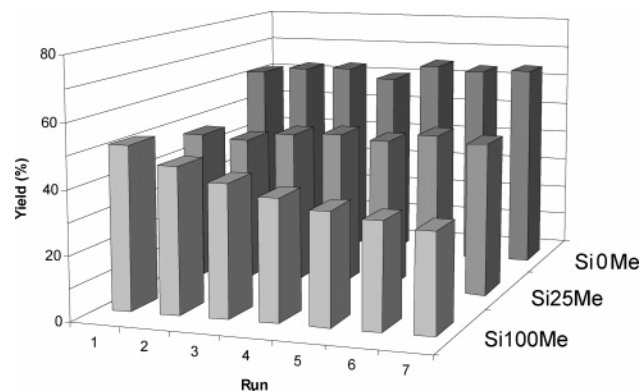


**Figure 5.** Yields in the NaOBr oxidation of 1-nonanol to give nonanal in the presence of TEMPO entrapped in silica (Si0Me, front row), and in ORMOSIL [Si25Me is 25% and Si100Me is 100% methylated (middle and back rows, respectively)].

freedom of the dopant molecule. Remarkably, in fact, an abrupt increase in the activity<sup>5,12</sup> of ORMOSIL-entrapped catalysts is observed exactly when six-member rings become largely predominant (above 75% MTMS).

Indeed, the chemical reactivity of sol–gel doped ORMOSIL is affected by another fundamental factor, namely, the flexibility<sup>14</sup> of the sol–gel cages that is known to be crucially affected by the employment of substituted silanes R'Si(OR)<sub>3</sub> in the sol–gel polycondensation, which largely diminishes the amount of hindering intracage hydrogen bonds between Si–OH groups and water (see below the EPR analyses).

Encapsulation within the organosilica cages, in its turn, impairs both chemical and physical stability to the (valuable) entrapped catalyst, which can then be recycled upon easy separation from the reaction mixture. Hence, while the unmodified silica-encapsulated TEMPO xerogel, Si0Me, lost half of its initial high activity upon just one oxidative run, turning its color to white as a clear indication of material dissolution and leaching of the radical in the reaction mixture, the 25% methyl-modified silica gel, Si25Me, shows a noteworthy stable activity, along with an unique *increment* in the intermediate yields upon the first three runs in which the catalyst was tested. Remarkably, this was also observed for the fully (100%) methylated gel, Si100Me, which after six runs was 8% more active than the fresh catalyst and showed the same pronounced stability (Figure 5).

These results indicate that in the heterogeneous NaOBr alcohol oxidations mediated by sol–gel ORMOSIL a *cooperative* mechanism is in action through which the more substrate (and product) molecules are adsorbed (and formed) within the inner cage surface, the faster the diffusion of the reactant (and product) molecules through the porous network<sup>15</sup> due to the fact that these materials are chemical *sponges* with chromatographic properties; i.e. they adsorb and concentrate the reagents at the cages surface where reactions take place, while the adsorbed molecules promote further diffusion of incoming reactants.

The homogeneous sol–gel encapsulation process disperses and protects the dopant species *within* the organosilica

(12) Reetz, M. T. *Adv. Mater.* **1997**, *9*, 943.

(13) De Witte, B. M.; Commers, D.; Uytterhoeven, J. B. *J. Non Cryst. Solids* **1996**, *202*, 35.

(14) Avnir, D. *Acc. Chem. Res.* **1995**, *28*, 328.

(15) An analogous explanation was invoked to rationalize the results of the adsorption properties of similar sol–gel organosilica xerogels in: Fireman-Shoresh, S.; Hüsing, N.; Avnir, D. *Langmuir* **2001**, *17*, 5958.

nanopores, thus preventing the continuous decrease in the activity of TEMPO anchored to commercial aminopropyl-silica (due to intermolecular quenching of the radicals anchored in proximity at the material surface).<sup>16</sup> In fact, surface material's derivatizations require the formation of a new covalent bond through a slow heterogeneous reaction that leaves the anchored molecules unprotected at the material pores surface.

In general, the sol-gel encapsulation results in synthetically important selectivity enhancement, a materials-science based advantage which *cannot* be achieved via classical homogeneous synthesis.<sup>18</sup> According to a general concept of heterogeneous catalysis, analogous to Fisher's "key-in-the-lock" mechanism explaining the selectivity of enzymatic reactions,<sup>17</sup> the spatial confinement in the narrow silica pores restricts the possible orientations that a reactant can assume when approaching the catalytic center, while the interaction between the substrate molecules and the alkyl groups at the cage surface (hindering free tumbling of the substrate molecule), dictates specific orientational approach to the catalyst. As a result, sol-gel entrapped catalysts show higher selectivity in comparison either to the catalyst in solution or surface-bound to a nonporous material.<sup>1,5</sup>

Hence, for instance, in the oxidative synthesis of aromatic amino hydroxy acids from aminodiols catalyzed by TEMPO, the heterogeneous oxidation over the hydrophobized silica matrix Si100Me results in 3-fold selectivity improvement compared to the homogeneous process,<sup>18</sup> while an analogous improvement in the synthesis of valuable  $\alpha$ -hydroxy acids from aromatic diols is observed using the same ORMOSIL in place of homogeneous TEMPO with a radical reduction of fragmentation product and a preferential yield of oxidized product.<sup>19</sup>

Incidentally, the EPR spectrum of ORMOSIL-entrapped TEMPO in Figure 6a shows, from the absence of spurious peaks (pointing to the presence of H<sub>2</sub>O molecules bond to silanols at the cage surface) compared to that of silica-entrapped TEMPO in Figure 6c, that the TEMPO moiety encapsulated in the organosilica cage enjoys largely enhanced freedom (from the absence of strong hydrogen bonding) and thus confirms the increased flexibility of the organosilica cage mentioned above.

Finally, the difference in the EPR spectra of silica-encapsulated and silica-supported TEMPO shows how different the sol-gel encapsulation of dopant molecules is as compared to adsorption at an external surface: Silica-supported TEMPO gives a broad low signal (Figure 6d) reflecting extensive intermolecular spin interactions among

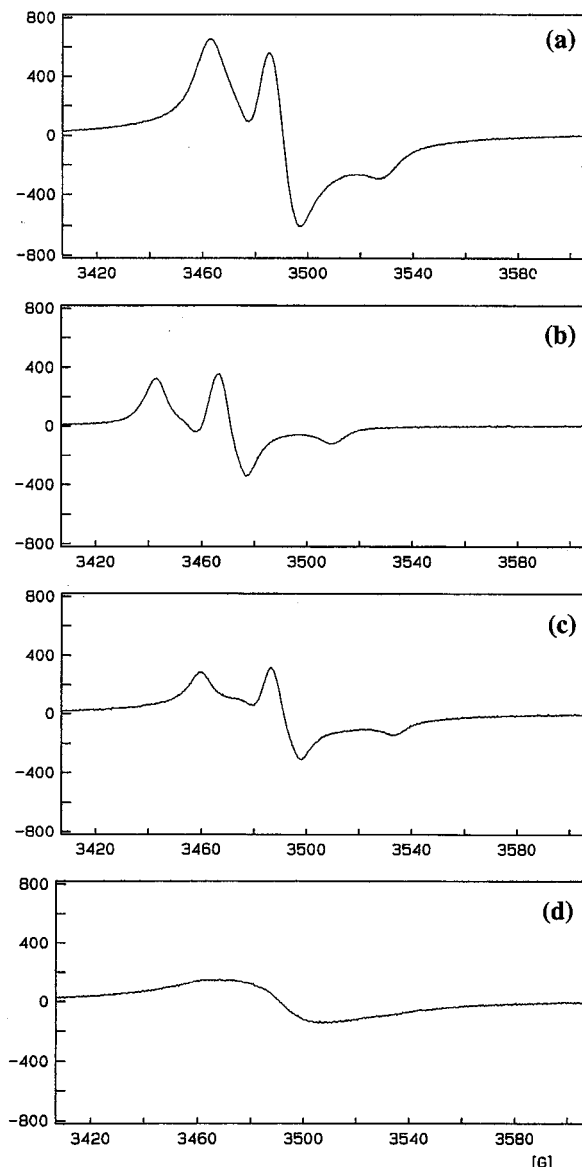


**Figure 6.** EPR spectra of sol-gel ORMOSIL doped with TEMPO Si50Me prior (a) and after (b) 7 consecutive reaction runs in the NaOBr oxidation of 1-nonanol. The spectra of sol-gel silica-entrapped (c) and surface-derivatized (d) TEMPO gels are shown for comparison.

the radicals anchored at the surface,<sup>20</sup> while the triplet shown by the encapsulated radicals (Figure 6c) reflects the *isolation* of the radicals within the sol-gel cages.

**Influence of the Alkyl Chain Length.** A similar trend of incremental reaction rates in the biphasic oxidation of alcohols was shown by the 75% propyl-modified silica (Si75Pr), which had an activity comparable to Si75Me, while the analogous 75% ethyl-modified gel (Si75Et) was considerably less active.<sup>6</sup> Propyl-modified xerogels, in fact, are as good as methyl-modified materials, and these are the materials that are commercialized along with methyl-modified analogues in the case of entrapped lipases.<sup>21</sup>

An attempt to correlate this behavior with the catalyst structure was made, by analyzing the structural influence imparted by different alkyl chain lengths. The DRIFT spectra of samples Si0Me, Si75Me, Si75Et and Si75Pr, normalized

(16) Fey, T.; Fischer, H.; Bachmann, S.; Albert, K.; Bolm, C. *J. Org. Chem.* **2001**, *66*, 8154.

(17) Jones, M. D.; Raja, R.; Thomas, J. M.; Johnson, B. F. G.; Lewis, D. W.; Rouzaud, J.; Harris, K. D. M. *Angew. Chem., Int. Ed.* **2003**, *42*, 4326. For several examples of enantioselectivity enhancement upon catalyst encapsulation, see the references cited in: Jacobi, M. *Chem. Eng. News* **2004**, *82* (11), 37.

(18) Testa, M. L.; Ciriminna, R.; Hajji, C.; Zaballos-Garcia, E.; Ciclosi, M.; Sepúlveda-Arques, J.; Pagliaro, M. *Adv. Synth. Catal.* **2004**, *6*, 655.

(19) Gancitano, P.; Ciriminna, R.; Testa, M. L.; Fidalgo, A.; Ilharco, L. M.; Pagliaro, M. *Org. Biomol. Chem.* **2005**, *3*, 2389.

(20) Shames, A.; Lev, O.; Iosefzon-Kuyavskaya, B. *J. Non-Cryst. Solids* **1994**, *175*, 14.

(21) For a series of commercially available ORMOSIL-entrapped lipases, see the 2005/2006 Fluka Catalogue of Reagents.

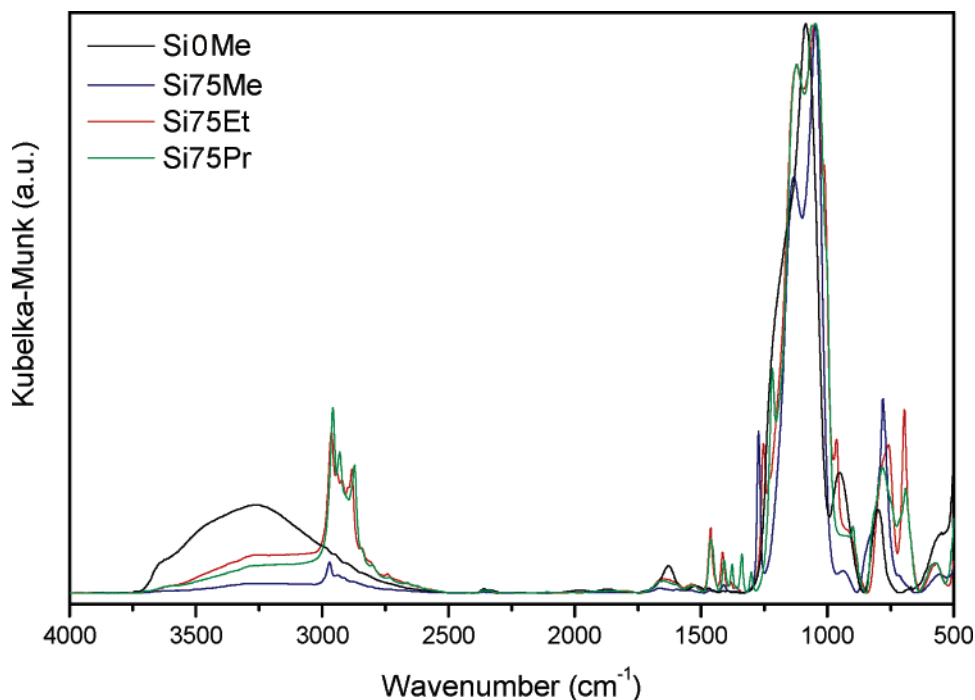


**Figure 7.** DRIFT spectra of silica- and ORMOSIL-entrapped TEMPO on going from methyl- to ethyl- and propyl-75%-modified xerogels (samples Si0Me, Si75Me, Si75Et, and Si75Pr).

to the maximum of the silica  $\nu_{\text{as}}\text{Si}-\text{O}-\text{Si}$  band, are compared in Figure 7.

In the high wavenumber region ( $2500\text{--}4000\text{ cm}^{-1}$ ), two interesting observations arise. The first one concerns the hydrophilicity of the samples: as expected, the modified catalysts are much less hydrophilic than the pure inorganic one, since the relative intensity of the  $\nu(\text{O}-\text{H})$  band is much lower. Among the modified catalysts, Si75Et is the more hydrophilic, since its spectrum shows the highest relative intensity of the  $\nu(\text{O}-\text{H})$  band. As the spectra of catalysts modified with ETMS and PTMS show the fingerprint of molecular water (the  $\delta(\text{H}-\text{O}-\text{H})$  mode, at  $\sim 1640\text{ cm}^{-1}$ ), the  $\nu(\text{O}-\text{H})$  band cannot be assigned exclusively to residual silanol groups, but also to adsorbed water. The highest relative intensity of the water  $\delta(\text{H}-\text{O}-\text{H})$  band in the catalyst modified with ETMS also points to a slightly higher hydrophilicity of this ORMOSIL. Consequently, the hydrophobicity does not seem to increase monotonically with the alkyl chain length.

The second observation concerns the relative intensities of the  $\nu_{\text{as}}(\text{CH}_3)$  modes: since all these samples have the same modifier content, the stable terminal methyl groups are in the same proportion. Therefore, the  $\nu_{\text{as}}((\text{Si})\text{CH}_3)$  band (at  $2972\text{ cm}^{-1}$  for sample Si75Me) and the  $\nu_{\text{as}}((\text{C})\text{CH}_3)$  bands (at  $2965\text{ cm}^{-1}$  for Si75Et and at  $2959\text{ cm}^{-1}$  for Si75Pr) should not be very different. However, their relative intensities (normalizing to the silica network) are comparable for samples Si75Et and Si75Pr, but much higher than for Si75Me. The explanation for this may lie on a lower efficiency of the sol-gel process as a whole, when the alkyl group is ethyl or propyl, leading to a relatively higher  $(\text{C})-\text{CH}_3$  residual content in comparison to the silica network that really forms. On the other hand, the efficiency of the hydrolysis step may be assessed through the relative intensity of the  $\nu_{\text{as}}((\text{O})\text{CH}_3)$  band: it is weak in the Si75Me spectrum

**Table 3. Deconvolution Results of the  $850\text{--}1300\text{ cm}^{-1}$  Spectral Region of the DRIFT Spectra of Samples Si0Me, Si75Me, Si75Et, and Si75Pr<sup>a</sup>**

	Si0Me	Si75Me	Si75Et	Si75Pr
alkyl residue (molar %)	0	75	75	75
% $(\text{SiO})_6$	15.3	84.0	85.4	85.6
% $\text{Si}-\text{O}_d$	12.6	2.0	3.5	3.0
SSA ( $\text{m}^2/\text{g}$ )	217	100	160	75
SPV ( $\text{cm}^3/\text{g}$ )	1.24	0.27	0.74	0.38

<sup>a</sup> Comparison with the specific pore volume (SPV) and specific surface area (SSA) from  $\text{N}_2$  sorption isotherms. Me = methyl; Et = ethyl; Pr = propyl.

(as observed above), it is not detected for Si75Pr, probably being overlapped with the broad  $\nu_{\text{as}}((\text{Si})\text{CH}_2)$  band, with maximum at  $2929\text{ cm}^{-1}$ , but it is clearly defined at  $2942\text{ cm}^{-1}$  for Si75Et. This fact points to an incomplete hydrolysis in all cases, more evident when the alkyl group is ethyl. Somehow, the ethyl-substituted modifier seems to have a different effect upon the hydrolysis yield than a shorter or a longer chain. This fact could be related to the possibility of the propyl radical having gauche conformers with reduced steric hindrance, more similar to methyl.

The low-wavenumber region of the DRIFT spectra (below  $1500\text{ cm}^{-1}$ ) becomes more complex as the alkyl chain length increases, due to an overlapping of the alkyl modes expected at  $1015\text{--}1020$ ,  $970$ , and  $\sim 750\text{ cm}^{-1}$  in sample Si75Et and at  $1065$  and  $\sim 750\text{ cm}^{-1}$  in Si75Pr. However, the deconvolution of the region between  $1300$  and  $900\text{ cm}^{-1}$  in Gaussian and Lorentzian profiles produced some interesting results. They are summarized in Table 3, in terms of the relative areas of the bands related to the six-member rings (% $(\text{SiO})_6$ ), and the Si-dangling oxygen groups (% $\text{Si}-\text{O}_d$ ), calculated in the same manner as for Table 2.

It becomes clear that, in terms of siloxane structural rings, the three ORMOSIL are not that different, all containing a large predominance of six-member rings (above 84%). The

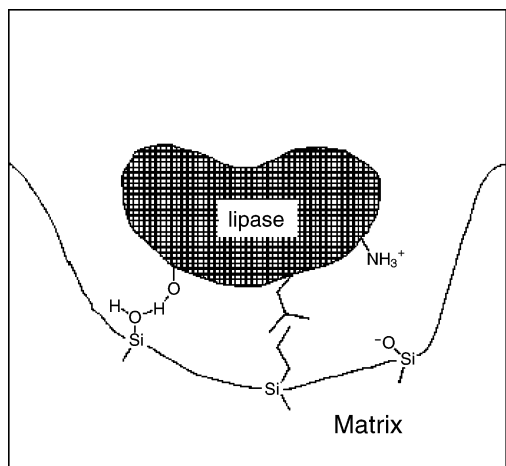


**Figure 8.** Noncovalent interactions between the gel matrix and the lipase according to Retz et al. (Reprinted with permission from ref 7. Copyright 2003 Wiley-VCH).

relative intensity of the  $\nu(\text{Si}-\text{O}_d)$  band, which is a measure of the condensation efficiency, has a maximum for the ethyl substituted modifier, in good agreement with the other sources of information on the hydrophilicity of the sample, and points to a less complete condensation in this case. The steric hindrance effect due to a more rigid ethyl group could again be called upon to justify this fact.

The quantification of lipophilicity was not made for samples Si75Et and Si75Pr, because the methylene bands overlap in the lowest spectral region, rendering deconvolution very unreliable. However, since the ethyl and propyl groups are stable (they do not participate in the sol-gel reactions), it is predictable that the lipophilicity increases in the order Si75Me, Si75Et, and Si75Pr. As a consequence, since the catalyst modified with ETMS is more hydrophilic and less lipophilic than the propyl-modified, and is much more hydrophilic and somewhat more lipophilic than the methyl modified, we may infer that it must have the highest HLB.

Interestingly, these findings correlate extremely well with the specific pore volume and specific surface areas of these catalysts, also included in Table 3: the one modified with ETMS, with highest HLB, has also the highest value of surface area and pore volume, as if its properties were more similar to the nonmodified catalyst than when the alkyl group is methyl or propyl. What is more important is that these properties may contribute to understanding the lowest reactivity of the ethyl-modified catalyst.

In conclusion, this analysis reveals that the important factors affording optimal catalytic performance are predominance of six-member rings (above 80% alkylation) and a low HLB. Investigators developing novel sol-gel catalysts will follow these guidelines to prepare optimal catalysts for relevant applications besides oxidation. Thus, for instance, considering that enzymes do not merely complement the transition states of the uncatalyzed reactions, but they rather enter into reactions with substrates by covalent bond formation,<sup>22</sup> in the case of entrapped lipases the schematic view of noncovalent interactions between the gel matrix and lipase enzyme (Figure 8) could well require revision, taking into

account the larger sol-gel cages and the electronic interaction between the organically modified cage and the enzyme active core.

Learning to master this interaction for different enzymes might thus lead to replication of the outstanding results obtained with entrapped lipase and is a challenge of paramount importance for organic synthesis on site-isolation catalysts.<sup>23</sup>

## Experimental Section

**Catalysts Preparation.** Methyltrimethoxysilane (MTMS), ethyltrimethoxysilane (ETMS), propyltrimethoxysilane (PTMS), 3-aminopropyl-trimethoxysilane (APTMS), tetramethylorthosilicate (TMOS), 4-oxo-2,2,6,6-tetramethyl-1-piperidinoloxo free radical (4-oxo-TEMPO), and methanol were purchased from Sigma-Aldrich and used without further purification. Ultrapure water (Millipore Type 1 quality) was used in all the preparations. The chemical entrapment of TEMPO moieties in the sol-gel silica hybrid materials was performed in two steps. The first step, the reductive amination of 4-oxo-TEMPO with APTMS, led to a TEMPO functionalized alkoxide that is then used in the subsequent sol-gel polycondensation process of MTMS and TMOS. Hence, xerogels derived from pure TMOS (Si0Me) and mixtures containing increasing amounts of MTMS were prepared (Table 1) up to an entirely methylated gel obtained from pure MTMS (Si100Me). Ethyl- and propyl-modified xerogels were obtained using the corresponding organosilanes in the sol-gel condensation. The chosen molar ratio was  $\text{Si}:\text{MeOH}:\text{H}_2\text{O} = 1:3:8$  for all the catalysts.

A typical catalytic ORMOSIL doped with TEMPO such as Si75Me was obtained dissolving APTMS (4 mmol) in MeOH (2.6 mL), lowering the pH at 7–8 and then adding 4-oxo-TEMPO (1 mmol) and  $\text{NaBH}_3\text{CN}$  (0.5 mmol). After 48 h under fast stirring at room temperature, the  $\text{NaBH}_3\text{CN}$  excess was destroyed adding HCl (49 mmol) and at the precursor mixture TMOS (1.750 mL), MTMS (4.370 mL), MeOH (2.730 mL), and  $\text{H}_2\text{O}$  (5.8 mL) were added under fast stirring. The sol gelled slowly and the alcogel thereby obtained was sealed, left to age at room temperature for 24 h and eventually dried at 60 °C for 5 days. The resulting elastic monolithic xerogel was eventually powdered and washed three times with DCM under reflux prior to drying at 60 °C. A typical catalytic load was 0.3 mmol of TEMPO/(g of catalyst) (an high and desirable load from industrial viewpoint).<sup>24</sup>

**Structural Characterization.** The sol-gel catalysts were structurally characterized by DRIFT spectroscopy, using a Mattson RS1 FTIR spectrometer with a Specac selector, in the range 4000 to 400  $\text{cm}^{-1}$  (with a wide band MCT detector), at 4  $\text{cm}^{-1}$  resolution. The spectra were the result of 500 co-added scans for each sample, ratioed against the same number of scans for the background (finely grinded KBr, FTIR grade). Surface area, pore volume, and pore size distributions were obtained by  $\text{N}_2$  sorption measurements at 77 K, on a Carlo Erba Sorptomatic 1900.

**General Oxidation Procedure with Si100Me as Catalyst.** The oxidations were performed in a glass tube with a cooling mantle equipped at the bottom with a ceramic filter plate that allowed easy

(23) Broadwater, S. J.; Roth, S. L.; Price, K. E.; Kobaslija, M.; McQuade, D. T. *Org. Biomol. Chem.* **2005**, *3*, 2899.

(24) For comparison, industry researchers recently reported 2.3 mmol  $\text{g}^{-1}$  of nitroxyl radical as a highly desirable high catalyst loading in the case of a polymer-supported TEMPO prepared by coupling 4-hydroxy-TEMPO onto functionalized polymer FibreCat (consisting of a fibre carboxylic acid functionalised via graft copolymerization, which results in a high density of active functional sites being generated on the polymer): Gilhespy, M.; Lok, M.; Baucherel, X. *Chem. Commun.* **2005**, 1085.

separation of the catalyst upon reaction. In a typical experiment the catalyst (30.0 mg, 8  $\mu$ mol of radical) was added to the tube followed by a  $\text{CH}_2\text{Cl}_2$  solution (2.0 mL) of the alcohol (0.4 M) with the internal standard dodecane (0.12 M) and 0.16 mL of aqueous KBr (0.5 M). After cooling the mixture to 0 °C, 2.7 mL of aq. NaOCl diluted to a concentration of 0.37 M and buffered by  $\text{NaHCO}_3$  to pH 9.1 were added and the resulting mixture shaken vigorously for 15 min. After filtration, the organic phase was separated, dried over  $\text{MgSO}_4$ , and the product analyzed by GC (ultra-2-column, HP). The filtered sol-gel catalyst was washed 5 times with  $\text{H}_2\text{O}$ , MeOH, and  $\text{CH}_2\text{Cl}_2$  (2 mL each), air-dried and reused as such in seven consecutive oxidation runs upon which the catalyst was used for the EPR measurements carried out at 296 K on a Bruker spectrometer working at medium frequency (50 kHz) and low-amplitude (0.101 G) modulation.

**Acknowledgment.** This paper is dedicated to the memory of Professor Tullio Agrigento and his fellow mates Pippo (Accascina) and Cesare (Carducci Artenisio). Thanks to the Quality College del Cnr for financial support.

**Note Added after ASAP Publication.** There were a number of errors in the version published ASAP November 24, 2005. Text changes were made to the abstract, Figures 1, 4, and 5 captions, Tables 1–3, the discussion of Figure 6, and the notation used to describe the characteristic vibrations of the  $\text{CH}_3$  group, and the labels in Figures 5 and 7 were modified. The corrected version was published ASAP December 1, 2005.

CM051954X